IMPACT: International Journal of Research in Engineering & Technology (IMPACT: IJRET)
ISSN(P): 2347-4599; ISSN(E): 2321-8843
Vol. 4, Issue 11, Nov 2016, 9-16

FORMABILITY OF ELLIPTICAL SS304 CUPS IN SINGLE POINT INCREMENTAL FORMING PROCESS BY FINITE ELEMENT METHOD

B. NAVYA SRI[1] & A. CHENNAKESAVA REDDY[2]

[1]Research Scholar, Department of Mechanical Engineering, JNT University, Hyderabad, India

[2]Professor, Department of Mechanical Engineering, JNT University, Hyderabad, India

ABSTRACT

The purpose of the present project work was to determine the formability of 304 stainless steel alloy to fabricate elliptical cups using single point incremental forming (SPIF) process. The finite element analysis has been carried out to model the single point incremental forming process using ABAQUS software code. The process variables of SPIF were sheet thickness, step depth, tool radius and coefficient of friction. The process parameters have been optimized using Taguchi techniques. The major process parameters influencing the SPIF of elliptical cups were sheet thickness, step size and tool radius.

KEYWORDS: 304 Stainless Steel, Elliptical Cup, Single Point Incremental Forming, Finite Element Analysis, Step Depth, Tool Radius, Sheet Thickness, Coefficient of Friction

INTRODUCTION

Formability is a function of sheet metal thickness and strain hardening. Formability is possible that specified sheet metal could be formed effectively into particular component or lead to fracture, depending upon the process conditions and the tooling used. Deep drawing is a compression-tension forming process [1, 2]. In a series of research on deep drawing process to fabricate variety of cup shapes, rich investigation have been carried out to improve the superplastic properties of materials such as AA2014 alloy [3], AA2219 alloy [4], AA2618 alloy [5], AA3003 alloy [6], Ti-Al-4V alloy [7], EDD steel [8] and gas cylinder steel [9]. In SPIF process, the sheet material is clamped along its edges and a hemispherical headed tool is moved along a predefined geometrical path so that it deforms the sheet locally along the path. The important process parameters, which influence the SPIF process capability, are tool diameter, step depth, feed rate, sheet thickness, lubrication, tool path and rotational speed of the spindle [10-15].

The present work was to study the formability of elliptical of 304 stainless steel using SPIF. For this purpose, the design of experiments was executed as per Taguchi technique. The process parameters of SPIF were sheet thickness, step depth, tool radius, and coefficient of friction. The formability was evaluated using finite element method.

MATERIAL AND METHODS

In the present work, ABAQUS (6.14) software code was used for the numerical simulation of SPIF process to fabricate elliptical cups. The material was 304 stainless steel. The SPIF process parameters were chosen at three levels as summarized in table 1. The orthogonal array (OA), L9 was preferred to carry out experimental and finite element analysis (FEA) as given in table 2.

Table 1: Process Parameters and Levels

Factor	Symbol	Level–1	Level–2	Level–3
Sheet thickness, mm	A	0.8	1.0	1.2
Step depth, mm	B	0.50	0.75	1.00
Tool radius, mm	C	4.0	5.0	6.0
Coefficient of friction	D	0.15	0.20	0.25

Table 2: Orthogonal Array (L9) and Control Parameters

Treat	A	B	C	D
1	1	1	1	1
2	1	2	2	2
3	1	3	3	3
4	2	1	2	3
5	2	2	3	1
6	2	3	1	2
7	3	1	3	2
8	3	2	1	3
9	3	3	2	1

The sheet and tool geometry were modeled as deformable and analytical rigid bodies, respectively, using ABAQUS. They were assembled as frictional contact bodies. The sheet material was meshed with S4R shell elements. The fixed boundary conditions were given to all four edges of the sheet. The boundary conditions for tool were x, y, z linear movements and rotation about the axis of tool. True stress-true strain experimental data were loaded in the tabular form as material properties. The tool path geometry, which was generated using CAM software [16], was imported to the ABAQUS as shown in figure 1. The elastic-plastic deformation analysis was carried out for the equivalent stress, strain and strain rates and thickness variation.

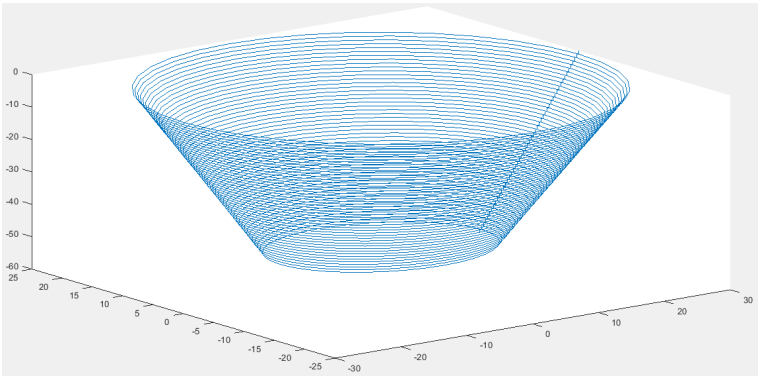

Figure 1: Tool Path Generation

RESULTS AND DISCUSSIONS

The influence of process variables on the von Mises stress, strain rate and thickness reduction are deliberated. The formability limit diagrams are also created.

Influence of Process Variables on Von Mises Stress

Table – 3 gives the ANOVA (analysis of variation) summary of von Mises stress data. The percent contribution specifies that sheet thickness, A, gives 3.90%, step depth, B, consensuses 60.13%, tool radius, C, grants 33.24% and

coefficient of friction, D, contributes 2.73% of total variation on the von Mises stress.

Table 3: ANOVA Summary of the Effective Stress

Source	Sum 1	Sum 2	Sum 3	SS	v	V	P
A	1487.93	1506.09	1535.05	376.52	2	188.26	3.90
B	1413.11	1599.44	1516.52	5809.86	2	2904.93	60.13
C	1536.78	1430.82	1561.47	3212.01	2	1606.00	33.24
D	1502.86	1494.10	1532.11	264.08	2	132.04	2.73
e				0.00	0		0.00
T	5940.69	6030.46	6145.16	9662.47	8		100.00

Note: *SS is the sum of square, v is the degrees of freedom, V is the variance, P is the percentage of contribution and T is the sum squares due to total variation.*

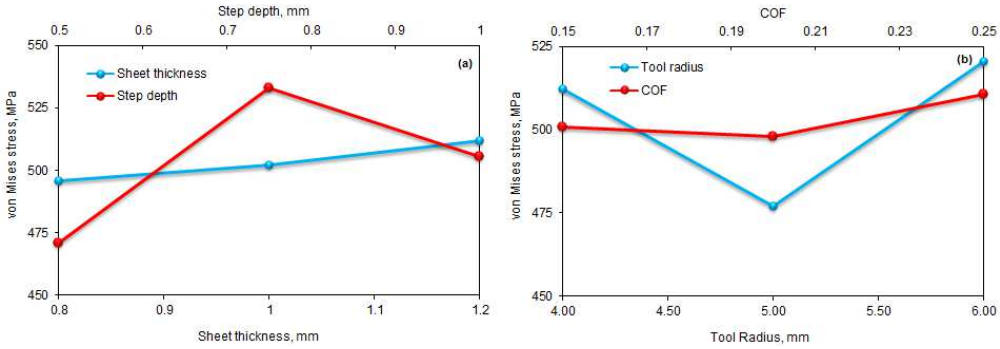

Figure 2: Influence of Process Parameters on Von Mises Stress

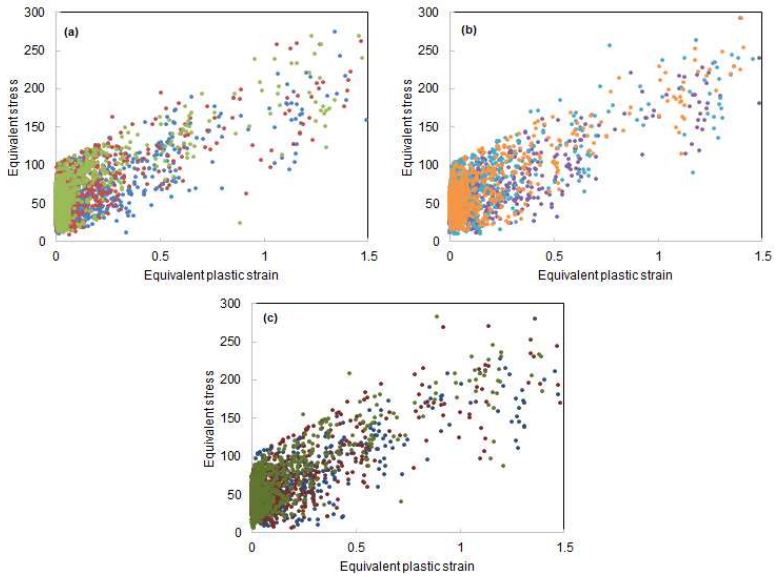

Figure 3: Effect of Equivalent Plastic Strain on Von Mises Stress

Figure 2 presents the influence of SPIF process parameters von Mises stress induced in 304 stainless steel. The von Mises stress was increased with increase of sheet thickness (figure 2a) as the force that need to apply for a given amount of elongation was influenced by the sheet thickness. In addition, figure 2a designates the von Mises stress as a function of step depth. The von Mises stress was found to high for step depth of 0.75 mm. The von Mises stress was found

to be minimum for tool radius of 5.0 mm as shown in figure 2b. Either above or below of this value, the von Mises stress was high. The effective stress increased with an increases in the coefficient of friction (figure 2b).

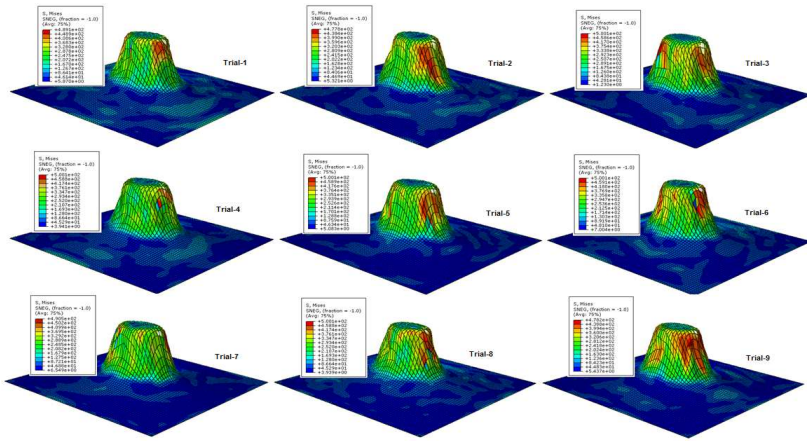

Figure 4: Raster Images of Von Mises Stress in the Cups

As observed from figure 3 that von Mises stress is directly proportional to equivalent plastic strain. For the trials 1, 2 and 3, the von Mises stresses were, respectively, 470.54 MPa, 494.41 MPa and 522.99 MPa. For the trials 4, 5 and 6, the von Mises stresses were, respectively, 451.02 MPa, 546.93 MPa and 508.14 MPa. For the trials 7, 8 and 9, the von Mises stresses were, respectively, 491.56 MPa, 558.10 MPa and 485.39 MPa. The ultimate tensile strength of 304 stainless steel is 505 MPa. The von Mises stress exceeded the tensile strength of 304 stainless steel for the trials 3, 5, 6 and 8 while it was lower than the tensile strength of 304 stainless steel for the trials 1, 2, 4 7 and 9 (figure 4).

Influence of Process Variables on Strain Rate

The ANOVA summary of the strain rate is given in Table 4. The percent contribution column establishes the major contributions 49.48%, 18.22%, 14.91% and 17.38% of sheet thickness, step depth, tool radius and coefficient of friction, respectively, towards variation in the strain rate.

Table 4: ANOVA Summary of the Strain Rate

Source	Sum 1	Sum 2	Sum 3	SS	v	V	P
A	0.3847349	0.180872	0.192137	0.0087534	2	0.0043767	49.48
B	0.2584297	0.3190128	0.1803015	0.0032239	2	0.001612	18.22
C	0.2089305	0.3246876	0.2241258	0.0026381	2	0.0013191	14.91
D	0.27	0.3085791	0.177033	0.0030752	2	0.0015376	17.38
e				2.776E-17	0		0
T	1.12	1.13	0.77	0.02	8		100.00

The strain rate was decreased with increase of sheet thickness (figure 5a) owing to the material availability for plastic deformation. As shown in figure 5a, the strain rate increased initially from 0.50 to 0.75 mm of step depth and later on, it decreased with further increase of step depth up to 1.00 mm. The magnitude of the step (Δz) down that the tool made after each pass was an important process variable, which had an effect on the strain rate responding to the elastic-plastic deformation of sheet. The effect of tool radius and coefficient of friction on strain rate are same as shown in figure 5b. The frictional shear stress is directly proportional to the coefficient of friction as per Coulomb's law of friction ($\tau = \mu F_n$, where

F_n is the normal pressure). When the frictional shear stress, reached the limiting shear stress of the sheet material, the material had undergone the plastic deformation. From this point, the frictional shear stress did not increase and had the value of the limiting shear stress and thereby limiting the coefficient of friction.

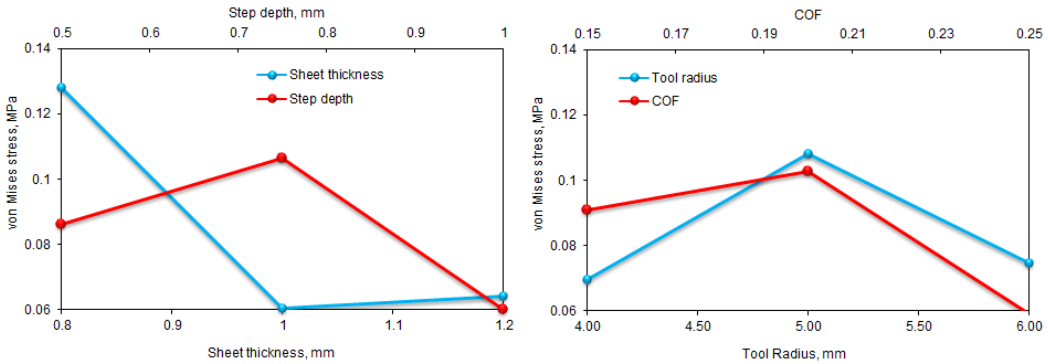

Figure 5: Influence of Process Parameters on Strain Rate

Influence of Process Variables on Thickness Reduction

The ANOVA summary of the thickness reduction is given in Table 5. In the decreasing order of contribution, sheet thickness, step depth, tool radius, and coefficient of friction accord, respectively, 71.24%, 13.31%, 14.57% and 0.88% towards variation in the thickness reduction.

Table 5: ANOVA Summary of the Thickness Reduction

Source	Sum 1	Sum 2	Sum 3	SS	v	V	F	P
A	0.48	0.61	0.74	0.01	2.00	0.0056	0.48	71.24
B	0.65	0.64	0.55	0.00	2.00	0.0010	0.65	13.31
C	0.66	0.62	0.55	0.00	2.00	0.0011	0.66	14.57
D	0.62	0.60	0.62	0.00	2.00	0.0001	0.62	0.88
e				0.00	0.00			0.00
T	2.41	2.46	2.46	0.02	8.00		2.41	100.00

The major process parameters, which influence the reduction of thickness, are initial sheet thickness, step depth and tool radius (figure 6). The reduction of sheet thickness was increased with increase of initial sheet thickness (figure 6a) attributed to the difference between input sheet thickness and the desired dimensions of the cup. The reduction of sheet thickness decreased with an increase in step depth (figure 6a). The reduction in thickness decreased with increase of tool radius as shown in figure 6b. The reduction of thickness was considered at the centerline of the deformed cup as shown in figure 7. As observed from figures 7, the majority of thickness reduction takes place in the walls of the cup but not in the flange or bottom of the cup. The elements located at the mid regions of the walls were elongated higher than those present at the top and bottom of the cup walls.

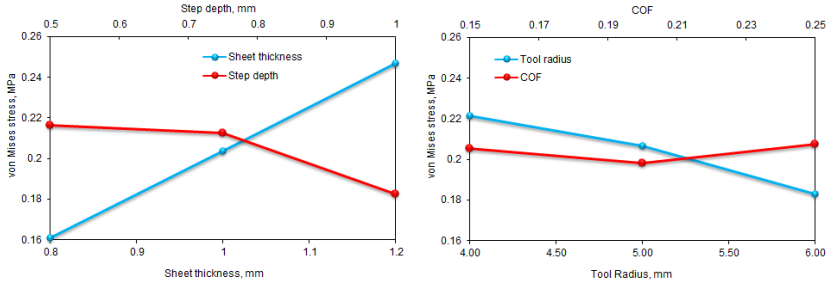

Figure 6: Influence of Process Parameters on Thickness Reduction

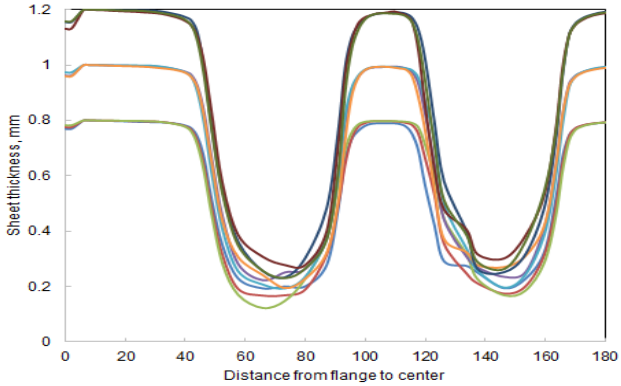

Figure 7: Location of Thickness Reduction in the Deformed Cup

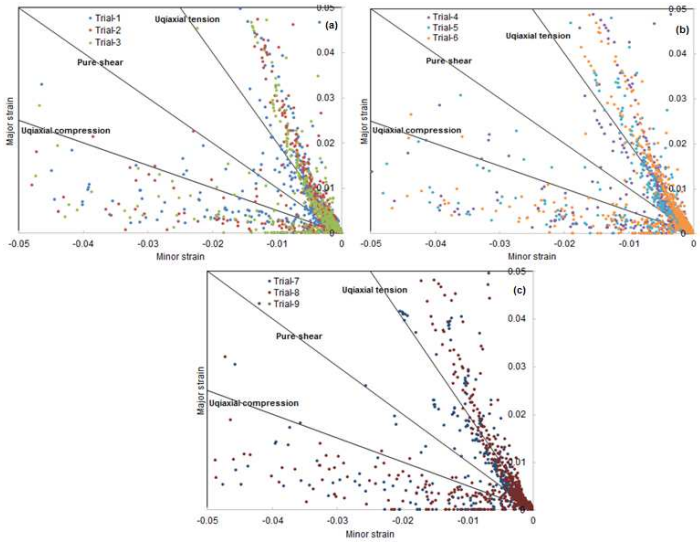

Figure 8: Forming Limit Diagrams (a) for Trials 1, 2, 3 (b) For Trials 4, 5, 6 (c) for Trials 7, 8, 9

Formability of SPIF Process

The formability diagrams of the cups are shown in figure 8. During initial stages of SPIF, the shear and compressive stresses were dominating the formability of elliptical cups of 304 stainless steel. At later stages of plastic deformation, the tension was highly predominant resulting the tension in the sheet. For all the trials, the major-axis side of the cup had experienced the compression and minor-axis side of the cup had accomplished the tension.

CONCLUSIONS

The major SPIF process variables, which could influence the formability of elliptical cups of 304 stainless steel, were sheet thickness, step depth and tool radius. The optimal process variables were sheet thickness of 1.0 mm, step depth of 0.5 mm, tool radius of 5.0 mm and coefficient of friction of 0.20.

REFERENCES

1. M.G. EI-Sebaie, “Plastic instability conditions when deep-drawing into a high pressure medium,” International Journal of Mechanical Sciences, 15, 605–615, 1973.
2. S. Yossifon, K. Sweeney, T. Altan, “On the acceptable blank holder force range in the deep drawing process,” Journal of Materials Processing technology, 67, 175–194, 2000.
3. A.C. Reddy, “Parametric Significance of Warm Drawing Process for 2024T4 Aluminum Alloy through FEA,” International Journal of Science and Research, 4 (5), 2345-2351, 2015.
4. A.C. Reddy, "Formability of High Temperature and High Strain Rate Superplastic Deep Drawing Process for AA2219 Cylindrical Cups," International Journal of Advanced Research, 3(10), 1016-1024, 2015.
5. A.C. Reddy, “High temperature and high strain rate superplastic deep drawing process for AA2618 alloy cylindrical cups,” International Journal of Scientific Engineering and Applied Science, 2, 2, 35-41, 2016
6. A.C. Reddy, "Practicability of High Temperature and High Strain Rate Superplastic Deep Drawing Process for AA3003 Alloy Cylindrical Cups," International Journal of Engineering Inventions, 5(3), pp. 16-23, 2016.
7. A.C. Reddy, "Finite element analysis of reverse superplastic blow forming of Ti-Al-4V alloy for optimized control of thickness variation using ABAQUS," Journal of Manufacturing Engineering, 1(1), 6-9, 2006.
8. A.C. Reddy, T. K. K. Reddy, M.Vidya Sagar, "Experimental characterization of warm deep drawing process for EDD steel," International Journal of Multidisciplinary Research & Advances in Engineering, 4(3), 53-62, 2012.
9. A.C. Reddy, “Evaluation of local thinning during cup drawing of gas cylinder steel using isotropic criteria,” International Journal of Engineering and Materials Sciences, 5(2), 71-76, 2012.
10. V. Srija, A. C. Reddy, “Numerical Simulation of Truncated Pyramidal Cups of AA1050-H18 Alloy Fabricated by Single Point Incremental Forming,” International Journal of Engineering Sciences & Research Technology, 5(6), 741-749, 2016.
11. T. Santhosh Kumar, A. C. Reddy, “Single Point Incremental Forming and Significance of its Process Parameters on Formability of Conical Cups Fabricated From AA1100-H18 Alloy, International Journal of Engineering Inventions,” 5(6), 10-18, 2016.
12. Raviteja, A. C. Reddy, “Implication of Process Parameters of Single Point Incremental Forming for Conical Frustum Cups From AA 1070 using FEA,” International Journal of Research in Engineering and Technology, 5(6), 124-129, 2016.
13. T. Santhosh Kumar, V. Srija, A. Ravi Teja, A. C. Reddy, “Influence of Process Parameters of Single Point

incremental Deep Drawing Process for Truncated Pyramidal Cups from 304 Stainless Steel using FEA," International Journal of Scientific & Engineering Research, 7(6), 100-105, 2016.

14. C.R. Alavala, "FEM Analysis of Single Point Incremental Forming Process and Validation with Grid-Based Experimental Deformation Analysis," International Journal of Mechanical Engineering, 5(5), 1-6, 2016.
15. C.R. Alavala, "Validation of Single Point Incremental Forming Process for Deep Drawn Pyramidal Cups using Experimental Grid-Based Deformation," International Journal of Engineering Sciences & Research Technology, 5(8), 481-488, 2016.
16. C.R. Alavala, "CAD/CAM: Concepts and Applications," New Delhi: PHI Learning Pvt. Ltd, 2008.